A Mathematical Model for a Dissolving Polymer

David A. Edwards and Donald S. Cohen
Applied Mathematics, California Institute of Technology, Pasadena, CA 91125

In certain polymer-penetrant systems, nonlinear viscoelastic effects dominate those of Fickian diffusion. This behavior is often embodied in a memory integral incorporating nonlocal time effects into the dynamics; this integral can be derived from an augmented chemical potential. The mathematical framework presented is a moving boundary-value problem. The boundary separates the polymer into two distinct states: glassy and rubbery, where different physical processes dominate. The moving boundary condition that results is not solvable by similarity solutions, but can be solved by perturbation and integral equation techniques. Asymptotic solutions are obtained where sharp fronts move with constant speed. The resultant profiles are quite similar to experimental results in a dissolving polymer. It is then demonstrated that such a model has a limit on the allowable front speed and a self-regulating mass uptake.

Introduction

In the last few years, new uses for polymers and other synthetic materials have revolutionized entire industries and created new ones, holding out promise for further outstanding advances. Polymeric adhesives adhere more while weighing less (Martuscelli and Marchetta, 1987; Shimabakuro, 1990; Pine, 1993). A "smart" polymer gel implanted in a diabetic can respond to high blood glucose levels and automatically introduce the needed dose of insulin (Travis, 1993). The use of polymer substrates for microlithographic patterning has emerged as a major industrial tool in very large-scale integration (VLSI) chip etching and elsewhere (Thompson et al., 1983). Polymer films are finding wide use in protective clothing, equipment, and sealants (Vrentas et al., 1975).

In many instances the exact physical mechanisms involved are still not understood. It is generally agreed that the standard Fickian flux $\tilde{J} = -D(\tilde{C})\nabla\tilde{C}$, where $D(\tilde{C})$ is the second-order diffusion tensor and $\tilde{C}$ is penetrant concentration, is not general enough to model the unusual phenomena these new materials exhibit. For instance, unless pathological conditions are met, a Fickian front always propagates with speed proportional to $\tilde{t}^{-1/2}$. However, in so-called "case II diffusion" in polymers, sharp concentration fronts often move with constant speed (Frisch et al., 1969; Tarche, 1991; Thomas and Windle, 1982). However, there is usually no discontinuity in $\tilde{C}$ at the phase transition as can be found in other more standard chemical systems (Crank, 1984).

Correspondence concerning this article should be addressed to D. A. Edwards, who is currently in the Department of Mathematics, University of Maryland, College Park, MD 20742.

There is a growing consensus that in these systems, some sort of viscoelastic stress plays a major role, sharing dominance with or robbing control from standard Fickian diffusion. The type of polymers we model are characterized by two distinct phases: *glassy* and *rubbery*. In the glassy state, the polymer has a finite *relaxation time* associated with the length of the polymer in relation to the entanglement network. This nonlocal effect is related to the "memory" of the polymer with respect to its concentration history. In the rubbery state, the polymer swells, making the relaxation time almost instantaneous. Hence, the "memory" of the polymer in the rubbery state is very faint (Vieth, 1991).

By using the ratio of the relaxation times as a dimensionless small parameter, we will construct asymptotic results that show that the inclusion of memory effects greatly changes the character of the solution. In the case of a polymer dissolving in the presence of a solvent, a sharp front of width on the order of the ratio of the relaxation times develops and moves with constant speed. Behind it, there is a region of finite width where the polymer changes from glass to rubber as it dissolves. At the end of this region is another sharp front that moves initially as t^2 and then with constant speed. At this point, the network disentangles and the concentration of the solvent increases greatly. These results closely mimic the experimental and numerical results of Peppas et al. (1994). Each of these behaviors is unobtainable with a standard Fickian model. We also derive another unusual result: *self-regulating mass uptake* in the dissolving polymer, where properties of the polymer determine the mass uptake in the system, re-

gardless of externally imposed boundary conditions. Such results mimic those found by Hui et al. (1987a).

Governing Equations

There is agreement that the classic Fickian diffusion equation $\tilde{C}_{\tilde{t}} = \nabla\cdot(D(\tilde{C})\nabla\tilde{C})$ cannot possibly describe experimental observations even when the diffusivity D is a nonlinear function of the concentration. This is not surprising when one realizes that in addition to molecular diffusion other fundamental physical processes are taking place (often yielding changes of phase).

The chief difficulty in deriving equations of motion is that the exact physical processes underlying the behavior of these materials are not well understood. Thus, any attempt to derive equations from the first principles of physics (mechanics, thermodynamics, etc.) require postulates or assumptions at some level. However, the most important and most commonly mentioned properties of glassy polymers all stem from finite mechanical relaxation times resulting from slow response to changing conditions. This observation suggests that although the interaction among the fundamental processes is not yet known, a global relaxation-type phenomenon can be utilized as a physical basis for a model (Frisch, 1980; Losi and Knauss, 1992; Paul and Koros, 1976; Thomas and Windle, 1982; Vieth and Sladek, 1965).

Our attempt to model this phenomenon is motivated by phenomenology and experimentally determinable parameters. Confidence is high in our model because it works in all cases so far (Cohen and White, 1989, 1991; Cox, 1988, 1990; Cox and Cohen, 1989; Edwards, 1994, 1995; Edwards and Cohen, 1995a,b; Hayes, 1990; Hayes and Cohen, 1992), and the mathematical structure used is strongly indicated by experiments and observations. We feel that if a true derivation from first principles (without assumptions) is ever possible, application to our problems will yield equations of the same form as we are using, and in fact, the few specific applications that have been studied are special cases of our theory. Our goal is the accurate description of the penetrant concentration (for either sorption or desorption). While the effects of other physical processes on the concentration field are accounted for, no attempt to track them is made here.

In relevant notation the classic Fick's diffusion equation comes about as follows. If $\tilde{C}$ represents the concentration of some diffusing species, and if $\tilde{U}$ is, in some sense, the internal energy of the system, then a chemical potential $\tilde{\mu}_F$ of the diffusing species is defined by

$$\tilde{\mu}_F = \frac{\delta\tilde{U}}{\delta\tilde{C}}.$$

A gradient of the potential $\tilde{\mu}_F$ will drive a current $\tilde{J}$ defined as

$$\begin{aligned}\tilde{J} &= -K(\tilde{C})\nabla\tilde{\mu}_F \\ &= -D(\tilde{C})\nabla\tilde{C},\end{aligned}$$

where the diffusivity $D(\tilde{C})$ is given by $D(\tilde{C}) = K(\tilde{C})\tilde{\mu}_F'(\tilde{C})$. The equation of conservation of mass then becomes

$$\frac{\partial\tilde{C}}{\partial\tilde{t}} = -\nabla\cdot\tilde{J} = \nabla\cdot[D(\tilde{C})\nabla\tilde{C}],$$

which is the classical Fickian diffusion equation.

For our more complicated polymer-penetrant problems, in addition to diffusive transport, various phenomena will contribute to the relaxation processes, which we now recognize with explicit dependence. That is, we let

$$\tilde{\mu} = \tilde{\mu}(\tilde{C}, \tilde{\sigma}),$$

where

$$\tilde{\sigma} = \int_0^{\tilde{t}}\left\{f\left[\tilde{C}(\tilde{x},\tilde{t}'),\tilde{C}_{\tilde{t}}(\tilde{x},\tilde{t}')\right]\right\}\exp\left\{-\int_{\tilde{t}'}^{\tilde{t}}\beta[\tilde{C}(\tilde{x},z)]\,dz\right\}d\tilde{t}'. \tag{1}$$

Here $\beta(\tilde{C})$ is the inverse of the relaxation time, which roughly corresponds to the time needed for one part of the polymer to respond to changes in neighboring parts, and $f(\tilde{C},\tilde{C}_{\tilde{t}})$ represents the functional dependence on the concentration field and its rate of change. Considerable discussion and reasoning goes into choosing appropriate forms for $\beta(\tilde{C})$ and $f(\tilde{C},\tilde{C}_{\tilde{t}})$ in analogous purely mechanical viscoelastic problems (Christensen, 1971; Cohen and White, 1991; Durning, 1985; Flugge, 1975). Forms appropriate for our problems are discussed in detail in Cohen et al. (1995), and a physically realistic intuition can be applied to choosing functional forms so that the models can be used for both descriptive and design purposes.

As earlier, the potential $\tilde{\mu}$ drives a flux $\tilde{J}$, now defined by

$$\tilde{J} = -\frac{\partial\tilde{\mu}}{\partial\tilde{C}}\nabla\tilde{C} - \frac{\partial\tilde{\mu}}{\partial\tilde{\sigma}}\nabla\tilde{\sigma}.$$

Thus, the basic equation of conservation of mass becomes

$$\frac{\partial\tilde{C}}{\partial\tilde{t}} = \nabla\cdot[D(\tilde{C})\nabla\tilde{C} + E(\tilde{C})\nabla\tilde{\sigma}], \tag{2}$$

where $E(\tilde{C}) = \partial\tilde{\mu}/\partial\tilde{\sigma}$.

For theoretical purposes the relaxation behavior inherent in Eq. 1 has appealing intuitive properties conforming to experimental observations. However, for actual analytical and numerical use in a given problem it is often preferable to note that $\tilde{\sigma}$ is the solution of the following equation:

$$\tilde{\sigma}_{\tilde{t}} + \beta(\tilde{C})\tilde{\sigma} = f\left(\tilde{C},\tilde{C}_{\tilde{t}}\right). \tag{3}$$

The simultaneous differential Eqs. 2 and 3 thus replace the integrodifferential equation system 1-2. It is shown in Cohen and White (1991) that while $\tilde{\sigma}$ can be thought of as a physical stress in one-dimensional problems, it is actually a nonstate variable used only as an artifice to simplify our equations.

This derivation implies the postulation of a generalized flux tensor of the form

$$\tilde{J}(\tilde{x},\tilde{t}) = -\sum_{n=1}^{\infty} D_n(\tilde{C})\nabla\int_{\Omega}\int_{-\infty}^{\tilde{t}} \mathfrak{F}_n[\tilde{C}(\tilde{x}',\tilde{t}')] \times \mathfrak{G}_n[\tilde{x}-\tilde{x}',\tilde{t}-\tilde{t}',\tilde{C}(\tilde{x}',\tilde{t}')]\, d\tilde{t}'\, d\tilde{x}', \quad (4)$$

where Ω is the region occupied by the polymer, the D_n are second-order tensors, the $\mathfrak{F}_n$ are general differential operators on $\tilde{C}$ that model the dependency of $\tilde{J}$ on different dynamical processes, and the $\mathfrak{G}_n$ are general nonlinear hereditary kernels. Each term in the expansion represents a flux contribution from a different source, such as molecular diffusion or viscoelasticity. Simplified versions of Eq. 4 have been studied by Cohen and his colleagues (Cohen et al., 1995; Cohen and White, 1989, 1991; Cox, 1988; Cox and Cohen, 1989; Edwards, 1994, 1995; Edwards and Cohen, 1995a,b; Hayes, 1990; Hayes and Cohen, 1992).

In many polymer-penetrant systems, $\beta(\tilde{C})$ changes greatly as the polymer goes from the glassy state to the rubbery state (Crank, 1976; Frisch, 1980; Hui et al., 1987a,b; Vieth, 1991). However, the differences in $\beta(\tilde{C})$ *within* phases are qualitatively negligible when compared with the differences *between* phases. Hence, we model $\beta(\tilde{C})$ by its average in each phase, yielding the following functional form:

$$\beta(\tilde{C}) = \begin{cases} \beta_g, & 0 \le \tilde{C} \le \tilde{C}_* \quad \text{(glass)} \\ \beta_r, & \tilde{C}_* < \tilde{C} \le \tilde{C}_c \quad \text{(rubber)}, \end{cases} \quad (5)$$

where $\tilde{C}_*$ is the concentration at which the rubber–glass transition occurs and $\tilde{C}_c$ is the saturation level for the polymer. Sub- and superscripts r refer to the rubbery region; sub- and superscripts g refer to the glassy region.

We now let f have a particularly simple form, so Eq. 3 becomes

$$\tilde{\sigma}_{\tilde{t}} + \beta(\tilde{C})\tilde{\sigma} = \eta\tilde{C} + \nu\tilde{C}_{\tilde{t}}, \quad (6)$$

where η and and ν are positive constants. More explanation of the dependence of stress on $\tilde{C}$ and $\tilde{C}_{\tilde{t}}$ can be found in Knauss and Kenner (1980), Cohen et al. (1995), and Fu and Durning (1993). We wish to model the penetration of solute imposed at the boundary of an initially dry one-dimensional semi-infinite polymer. By using a semiinfinite interval, we are able to ignore effects of polymer swelling on the system, which complicate the analysis of finite-domain problems (Peppas et al., 1994). This penetration will cause the polymer entanglement network to dissolve. Here $\tilde{C}$ is the concentration of the solvent. The polymer is dry initially, and an initial condition for $\tilde{\sigma}$ is given by Eq. 4:

$$\tilde{C}(\tilde{x},0) = 0, \quad \tilde{\sigma}(\tilde{x},0) = 0. \quad (7)$$

We wish to solve Eqs. 2 and 6 subject to Eq. 7. We want to incorporate effects of both the glassy and rubbery phases in our nondimensionalizations; hence we normalize $\tilde{x}$ by our diffusive length scale in the glassy region and $\tilde{t}$ by the relaxation time in the rubbery region. We nondimensionalize concentration by $\tilde{C}_c$ and $\tilde{\sigma}$ by $\nu\tilde{C}_c$. Letting $D(\tilde{C})$ and $E(\tilde{C})$ be constants, we have

$$x = \tilde{x}\sqrt{\frac{\beta_g}{D}}, t = \tilde{t}\beta_r, C(x,t) = \frac{\tilde{C}(\tilde{x},\tilde{t})}{\tilde{C}_c}, \quad \sigma(x,t) = \frac{\tilde{\sigma}(\tilde{x},\tilde{t})}{\nu\tilde{C}_c}, C_* = \frac{\tilde{C}_*}{\tilde{C}_c}. \quad (8)$$

Then Eqs. 2, 6, and 7 reduce to

$$C_t = \frac{\beta_g}{\beta_r}C_{xx} + \frac{\nu E\beta_g}{D\beta_r}\sigma_{xx}, \quad (9a)$$

$$\sigma_t + \frac{\beta(C)}{\beta_r}\sigma = \frac{\eta}{\nu\beta_r}C + C_t, \quad (9b)$$

$$C(x,0) = 0, \quad \sigma(x,0) = 0. \quad (10)$$

Since $\beta(C)$ is constant on either side of the threshold level $C = C_*$, we may combine Eqs. 9 to yield

$$C_{tt} = \frac{\beta_g(1+\gamma)}{\beta_r}C_{xxt} - \frac{\beta(C)}{\beta_r}C_t + \frac{\beta_g}{\beta_r^2}\left[\beta(C) + \frac{\eta E}{D}\right]C_{xx}, \quad (11)$$

where $\gamma = \nu E/D$. It can be shown that Eq. 11 also holds for σ.

Imagine an experiment in which a polymer matrix is exposed to a infinite well of diluent. Though the concentration of the diluent may be 1 at the edge of the polymer matrix, it is clear that at the *instant* that we introduce the polymer into the solvent, the concentration can be no greater than C_*, which is now defined as that concentration at which the entanglement network dissolves. We would expect that the maximal concentration of the diluent at the boundary will be achieved only in the mathematical limit $t \to \infty$. This motivates our boundary condition

$$C(0^+,t) = 1 - (1 - C_*)e^{-rt}, \quad (12)$$

where r is an $O(1)$ constant. Equation 12 can also be interpreted as a simplification of the surface boundary condition given in Hui et al. (1987a).

Our problem will involve matching the solutions in the two regions where $\beta = \beta_g$ and $\beta = \beta_r$. Thus, it is necessary to impose conditions at the moving boundary $s(t)$ between the two phases. First, it is clear that since $C_* < 1$, our front has an initial condition $s(0) = 0$. In polymer-penetrant systems, one does not see a *jump* in concentration, but rather a sharp rise at a moving front (Thomas and Windle, 1982). However, the front is still relatively wide when compared with molecular length scales, so the continuum model we use is still valid. Since there is no jump in concentration, C should be continuous at the front at the specified transition value C_*. In addition, we require that the phase transition be *complete* at this point (Alfrey et al., 1966), so we have

$$C^r[s(t),t] = C_* = C^g[s(t),t], C_t[s(t),t] > 0. \quad (13)$$

We also need a condition for the stress at the front. We follow the work of Knauss and Kenner (1980), where the derivative of stress with respect to a state variable has a jump in slope at the phase transition, but the actual stress is continuous:

$$\sigma^r[s(t),t] = \sigma^g[s(t),t]. \tag{14}$$

Lastly, we need a relationship between the flux $\tilde{J}$ at the front and the speed at which the front travels. Edwards (1995) has shown that a reasonable condition to impose is

$$[\tilde{J}]_{\tilde{s}} = -a\frac{d\tilde{s}}{d\tilde{t}}.$$

Edwards and Cohen (1995a) have also shown that the form of this equation is motivated by considering a flux condition analogous to that in the Stefan problem, where part of the flux is used up in the phase transition. Edwards (1995) has shown that it follows that

$$(D+\nu E)[C_x]_s + \nu E\left(\frac{\beta_g}{\beta_r}-1\right)\frac{\sigma[s(t),t]}{\dot{s}} = \frac{aD\beta_r}{\beta_g}\dot{s}. \tag{15}$$

Further discussion and the derivation of Eq. 15 may be found in Edwards (1994, 1995) and Edwards and Cohen (1995a).

The method of similarity solutions cannot be used to solve this moving boundary-value problem, and we need to tackle the entire set of partial differential equations in order to get results. To get analytical results from which we can track parameter dependence, we now wish to solve these equations using perturbation methods.

A Perturbation Approach

We exploit the fact that $\beta_g \ll \beta_r$ and define $\epsilon \equiv \beta_g/\beta_r$, where $0 < \epsilon \ll 1$. In the systems we wish to examine, the effects of stress dominate, so we set $\eta = \eta_0\epsilon^{-2}$. Making these substitutions into Eqs. 11 and 9b, we have two sets of equations, depending on the region of the polymer:

$$C^g_{tt} = \alpha\epsilon C^g_{xxt} - \epsilon C^g_t + (\epsilon^2+\kappa^2)C^g_{xx}, \tag{16a}$$

$$C^r_{tt} = \alpha\epsilon C^r_{xxt} - C^r_t + (\epsilon+\kappa^2)C^r_{xx} \tag{16b}$$

$$\sigma^g_t + \epsilon\sigma^g = \frac{\kappa^2}{\gamma}C^g + C^g_t, \quad \sigma^r_t + \sigma^r = \frac{\kappa^2}{\gamma}C^r + C^r_t, \tag{17a,b}$$

where $\kappa^2 = \eta_0 E/\beta_g D$ and $\alpha = 1+\gamma$. In addition, Eq. 15 becomes

$$[(D+\nu E)C_x]_s + \nu E(\epsilon-1)\frac{\sigma[s(t),t]}{\dot{s}} = \frac{aD}{\epsilon}\dot{s}, \tag{18}$$

and Eq. 9a becomes

$$C_t = \epsilon C_{xx} + \gamma\epsilon\sigma_{xx}. \tag{19}$$

We postulate the following expansions for C and σ in ϵ:

$$C = C^0 + o(1), \quad \sigma = \epsilon^{-1}\sigma^0 + o(\epsilon^{-1}).$$

Substituting these expressions and retaining only leading order terms in Eqs. 16–19, we have

$$C^{0g}_{tt} = \kappa^2 C^{0g}_{xx}, \qquad C^{0r}_{tt} + C^{0r}_t = \kappa^2 C^{0r}_{xx}, \tag{20a,b}$$

$$\sigma^{0g}_t = \frac{\kappa^2}{\gamma}\sigma^{0g}, \qquad \sigma^{0r}_t + \sigma^{0r} = \frac{\kappa^2}{\gamma}C^{0r}, \tag{21a,b}$$

$$\alpha\epsilon[C^0_x]_s - \gamma\frac{\sigma^0(s(t),t)}{\dot{s}} = a\dot{s}, \tag{22}$$

$$C^0_t = \gamma\sigma^0_{xx}. \tag{23}$$

If there is no boundary layer in the concentration to balance the stress term in Eq. 22, we see that $a < 0$. Therefore, a cannot be considered as directly analogous to a latent heat. This result may seem odd at first, but recall that we have now defined our total flux to include the gradient of the stress. Hence, even though the jump in the *concentration* flux may be positive at the front, the jump in the *total* flux may not be.

To solve Eqs. 20–23, we adopt the integral method used by Boley (1961). Thus, we introduce new quantities T^c and T^σ, which extend our equations to the fully semi-infinite region; quantities that must satisfy *fictitious* boundary conditions where they are not defined in the true problem. We indicate our unknown Dirichlet conditions by the following:

$$T^c(x,0) = C_u(x), \quad T^\sigma(x,0) = 0, \tag{24}$$

where the second condition follows from our definition of stress. From Eqs. 21b and 23, we have the Neumann boundary conditions:

$$T^\sigma_t(x,0) = \frac{\kappa^2}{\gamma}C_u(x), \quad C^{0r}_t(x,0) = 0. \tag{25}$$

We may also solve for the stress at the boundary using Eq. 21b:

$$\sigma^{0r}(0,t) = \frac{\kappa^2}{\gamma}\left\{1 - e^{-t} + \frac{1-C_*}{1-r}[e^{-t} - e^{-rt}]\right\}, \quad r \neq 1. \tag{26}$$

We now extend our equations to the entire semi-infinite region. Hence, we have

$$T^c_{tt} = \kappa^2 T^c_{xx} - T^c_t, \quad T^\sigma_{tt} = \kappa^2 T^\sigma_{xx} - T^\sigma_t, \quad 0 < x < \infty \tag{27a,b}$$

$$T^c = C^{0r}, \qquad T^\sigma = \sigma^{0r}, \qquad 0 < x < s(t) \tag{28a,b}$$

$$T^c(0,t) = 1 - (1-C_*)e^{-rt}, \tag{29}$$

$$s(0) = 0. \tag{30}$$

The solution of Eqs. 24, 25, 27a, and 29 can be written as $T^c = T^{ck}H(\kappa t - x) + T^{cu}$, where $H(\cdot)$ is the Heaviside step function. Here T^{ck} is the part of the solution arising from the boundary condition:

$$T^{ck}(x,t)=\frac{x}{2}\int_{x/\kappa}^{t} e^{-z/2}[1-(1-C_*)e^{-r(t-z)}-C_u(0)]\times\frac{I_1\left(\sqrt{\kappa^2z^2-x^2}/2\kappa\right)}{\sqrt{\kappa^2z^2-x^2}}\,dz+[1-(1-C_*)e^{-r(t-x/\kappa)}-C_u(0)]e^{-x/2\kappa},\quad(31)$$

where $I_1(\cdot)$ is the first modified Bessel function. T^{cu} is the part of the solution arising from the Dirichlet initial condition:

$$T^{cu}(x,t)=C_u(x)+\kappa\int_0^t[C_u'(x+\kappa z)-C_u'(|x-\kappa z|)]g_u(z,t)\,dz,\quad(32a)$$

where

$$g_u(z,t)=\left[\frac{e^{-z/2}}{2}+\frac{z}{4}\int_z^t e^{-y/2}\frac{I_1\left(\sqrt{y^2-z^2}/2\right)}{\sqrt{y^2-z^2}}\,dy\right]H(t-z).\quad(32b)$$

Similarly, the solution of Eqs. 24–27a is $T^{\sigma}=T^{\sigma k}H(\kappa t-x)+T^{\sigma d}$, where

$$T^{\sigma k}(x,t)=\frac{x}{2}\int_{x/\kappa}^{t} e^{-z/2}T^{\sigma}(0,t-z)\frac{I_1\left(\sqrt{\kappa^2z^2-x^2}/2\kappa\right)}{\sqrt{\kappa^2z^2-x^2}}dz+T^{\sigma}(0,t-x/\kappa)e^{-x/2\kappa},\quad(33)$$

and $T^{\sigma d}$ is the part of the solution arising from the Neumann condition:

$$T^{\sigma d}=\begin{cases}\dfrac{e^{-t/2\kappa}}{2\gamma}\displaystyle\int_{x-\kappa t}^{x+\kappa t}C_u(z)g_d(x-z,t)dz, & x>\kappa t\\[2ex] \dfrac{e^{-t/2\kappa}}{2\gamma}\left[\displaystyle\int_0^{x+\kappa t}C_u(z)g_d(x-z,t)dz-\int_0^{\kappa t-x}C_u(z)g_d(x+z,t)\,dz\right], & x<\kappa t,\end{cases}\quad(34a)$$

where

$$g_d(y,t)=I_0\left(\sqrt{\kappa^2t^2-y^2}/2\kappa\right).\quad(34b)$$

Our system is now completely described by Eqs. 31–34.

Self-Regulating Mass Uptake in a Dissolving Polymer

Now we will derive the interesting result that r is determined by the material properties of the entanglement network. Thus, there is actually a *self-regulating mass uptake* at the boundary. We expect that the dominant mechanism by which the front moves is the release of stress accumulated in the entanglement network (Alfrey et al., 1966). As the polymer dissolves, the increase in stress is reduced, which forces the front forward. Hence, we expect $[\sigma_x]_s$ to be so negative that $a<0$. For reasons that will become clear later we wish to restrict a to the following range:

$$-1\le a\le -C_*.\quad(35)$$

Since Eq. 20a is a hyperbolic equation and our initial condition is $C^{0g}(x,0)=C_t^{0g}(x,0)=0$, we see that for $x>\kappa t$ the solution is exactly 0, unless there is a boundary layer in that region, which our choice of a in Eq. 35 precludes. Hence, we expect there to be a discontinuity around the line $x=\kappa t$. For a first guess, we assume that $C(\kappa t^-,t)>C_*$. This means that our glass–rubber interface is hidden in a boundary layer around $x=\kappa t$. However, this leads to an unresolvable contradiction, and so we conclude that $s(t)<\kappa t$. Therefore, we will call the line $x=\kappa t$ the *primary front*, since it is the first signal to reach a certain point. We define the *secondary front* $x=s(t)$ to be the curve where the network is completely dissolved. We see from Eq. 20a that characteristics carry some constant value C_k forward with speed κ, so there must exist a "mushy region" $s(t)<x<\kappa t$ where $C\equiv C_k$. This is illustrated in Figure 1, which is our solution in the $x-t$ plane.

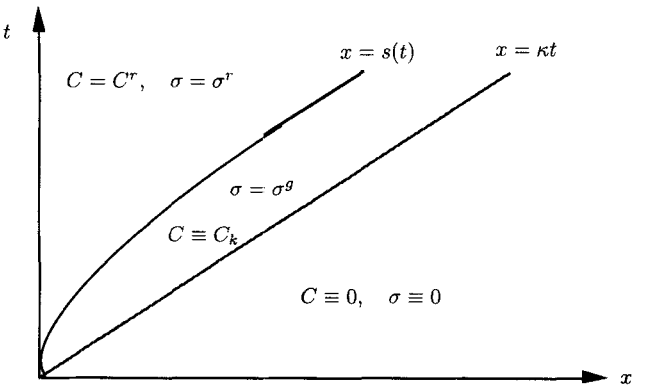

Figure 1. Regions of validity for different outer representations.

In order to retain our smoothing internal layer around $x=\kappa t$, we introduce the following scalings:

$$\zeta=\frac{x-\kappa t}{\epsilon^{1/2}},\ \tau=t,\ C^g(x,t)=C^{0+}(\zeta,\tau)+o(1),\quad(36)$$

where the exponent on ϵ has been chosen to yield a domi-

nant balance. Making these substitutions in Eq. 16a, we have

$$-2C^{0+}_{\zeta\tau} = -\alpha C^{0+}_{\zeta\zeta\zeta}, \tag{37}$$

where we now have the initial condition

$$C^{0+}(\zeta,0) = C_\kappa H(-\zeta). \tag{38}$$

Equation 37 is simply the diffusion equation for C^{0+}_ζ on an unbounded interval. The solution is

$$C^{0+}(\zeta,\tau) = \frac{C_k}{2}\operatorname{erfc}\left(\frac{\zeta}{\sqrt{2\alpha\tau}}\right), \tag{39}$$

where we have used Eq. 38. In order to determine C_k, we first look for a boundary layer in C^{0g} around our secondary front. This again leads to a contradiction. Thus, there is no layer in C^{0g} and C_k must equal C_*.

Next we solve for σ, which is immediately found from Eq. 21a:

$$\sigma^{0g}(x,t) = \frac{\kappa^2 C_*}{\gamma}\left(t - \frac{x}{\kappa}\right)H(\kappa t - x). \tag{40}$$

Hence, in order for σ^{0g} to stay bounded (which is what we expect both on physical and mathematical grounds), we see that

$$s(t) \sim \kappa t - s_\infty + s_1(t) \text{ as } t \to \infty, \tag{41}$$

where $s_\infty > 0$ and $s_1(t) \to 0$ as $t \to \infty$. Using Eq. 40 evaluated at our secondary front, we see that Eq. 22 becomes

$$\alpha\epsilon[C^0_x]_s - \frac{\kappa^2 C_*}{\dot{s}}\left[t - \frac{s(t)}{\kappa}\right] = a\dot{s} \tag{42}$$

In addition, we must solve *one* of the following two sets of conditions. If there is no boundary layer, then we have two conditions at the front that are given by Eqs. 13 and 42. However, it can be shown that with two constraints the problem is overdetermined. Therefore, there must be a boundary layer in C^{0r} around our secondary front. Introducing the following scalings:

$$\zeta = \frac{x - s(t)}{\epsilon}, \quad C^r(x,t) = C^{0-}(\zeta,t) + o(1),$$

into Eq. 16b, we have

$$\dot{s}^2 C^{0-}_\zeta = -\alpha\dot{s}C^{0-}_{\zeta\zeta\zeta} + \kappa^2 C^{0-}_{\zeta\zeta},$$

the solution of which is

$$C^{0-}(\zeta,\tau) = C^{0r}[s(t),t] + \{C_* - C^{0r}[s(t),t]\}\exp\left[\frac{(\kappa^2 - \dot{s}^2)\zeta}{\alpha\dot{s}}\right], \tag{43}$$

where we have used Eq. 13.

Then, using Eq. 43, Eq. 42 becomes

$$\{C^{0r}[s(t),t] - C_*\}(\kappa^2 - \dot{s}^2) - \kappa^2 C_*\left[t - \frac{s(t)}{\kappa}\right] = a\dot{s}^2. \tag{44}$$

Note there is no condition associated with Eq. 13.

In the next section we will construct asymptotic solutions for large and small t.

Asymptotic Analysis

Now we find asymptotic estimates for large t. To do this, we will need the result that

$$F(t) = \int_0^{s+\kappa t} f(z) I_0\left[\sqrt{\kappa^2 t^2 - (s-z)^2}/2\kappa\right] dz \sim 2\kappa f(\kappa t)e^{t/2}. \tag{45}$$

This follows from using Laplace's method (Bender and Orszag, 1978) and the asymptotic expansion for the Bessel function (Abramowitz and Stegun, 1972).

The other terms in T^σ are exponentially decaying, so Eq. 34 becomes

$$T^\sigma(s,t) \sim \frac{e^{-t/2}\kappa}{2\gamma}[2\kappa C_u(\kappa t)e^{t/2}]. \tag{46}$$

Using Eqs. 46, 40 and 41 in Eq. 14, we have

$$\frac{\kappa^2}{\gamma}C_u(\kappa t) \sim \frac{\kappa^2 C_*}{\gamma}\left[t - \frac{\kappa t - s_\infty}{\kappa}\right]. \tag{47}$$

To construct our solutions for long time, we postulate the following expansion for large x:

$$C_u(x) \sim C_\infty + o(1),$$

from which we have

$$C_\infty \sim \frac{C_* s_\infty}{\kappa}, \quad \sigma^{0r}[s(t),t] \sim \frac{\kappa C_* s_\infty}{\gamma}. \tag{48}$$

For T^c, all terms but the first in Eq. 32a are exponentially decreasing, so we have

$$T^c(s,t) \sim C_u(\kappa t) \quad \text{and} \quad T^c(s,t) \sim \frac{C_* s_\infty}{\kappa},$$

which yield

$$s_\infty = \frac{|a|\kappa}{C_*}, \quad C^{0r}[s(t),t] \sim |a|. \tag{49}$$

From the fact that $C_* \le C^{0r} \le 1$ we have our compatibility condition Eq. 35. Physically, we see that if the absolute jump in flux needed to move the front is too small, the front will try to move faster than κt. In addition, if the absolute jump in the flux needed is larger than the saturation concentration (in some appropriate nondimensionalization), the front cannot move at all. Thus, the mathematical model has a deficiency that we believe reflects a physical phenomenon, in the same way that the Fickian model is mathematically unstable for nonphysical negative diffusion coefficients.

Summarizing our results, we have the following:

$$C^{0g}(x,t) = \frac{C_*}{2}\,\mathrm{erfc}\left(\frac{x-\kappa t}{\sqrt{2\alpha\epsilon t}}\right), \tag{50a}$$

$$\sigma^{0g}(x,t) = \frac{\kappa^2 C_*}{\gamma}\left(t - \frac{x}{\kappa}\right)H(\kappa t - x), \tag{50b}$$

$$C^{0r}(x,t) = T^c(x,t) + \{C_* - T^c[s(t),t]\} \times \exp\left\{\frac{(\kappa^2 - \dot{s}^2)[x-s(t)]}{\alpha\epsilon\dot{s}}\right\}, \tag{50c}$$

$$t \to \infty, \quad 0 \ll x < \kappa t, \quad s(t) \sim \kappa t - \frac{|a|\kappa}{C_*}, \tag{51a}$$

$$T^c(x,t) \sim |a| + [1-(1-C_*)e^{-r(t-x/\kappa)}]e^{-x/2\kappa} + \frac{x}{2}\int_{x/\kappa}^{t} e^{-z/2}[1-(1-C_*)e^{-r(t-z)}]\frac{I_1\left(\sqrt{\kappa^2 z^2 - x^2}/2\kappa\right)}{\sqrt{\kappa^2 z^2 - x^2}}\,dz, \tag{51b}$$

$$\sigma^{0r}(x,t) \sim \frac{x}{2}\int_{x/\kappa}^{t} e^{-z/2}T^\sigma(0,t-z)\frac{I_1\left(\sqrt{\kappa^2 z^2 - x^2}/2\kappa\right)}{\sqrt{\kappa^2 z^2 - x^2}}\,dz + T^\sigma(0,t-x/\kappa)e^{-x/2\kappa} + \frac{\kappa|a|e^{-t/2}}{2\gamma}\int_{-\kappa t}^{\kappa t} g_d(z,t)\,dz. \tag{51c}$$

Figure 2 shows our large-time asymptotic expansion of C for a selected set of parameter values that satisfies Eq. 35. Though not quite so pronounced for $t = 6$, we see the three-stage concentration profile we predicted. The concentration profile starts out at 0, rises quickly to C_* at the primary front, remains at C_* in the mushy region, which for large time is of constant finite width, rises quickly to $|a|$ at $s(t)$, and then slowly rises for $x < s(t)$. These sharp fronts are commonly seen in polymer-penetrant systems (Alfrey et al., 1966; Hui et al., 1987b; Peppas et al., 1994), and three-stage profiles also have been observed (Herman and Edwards, 1990). Since these concentration profiles are good only for $x \to \infty$, we see that they rise above 1 as $x \to 0$. We would then expect the true concentration profile to depart from our long-time asymptotics and converge to 1 at $x = 0$.

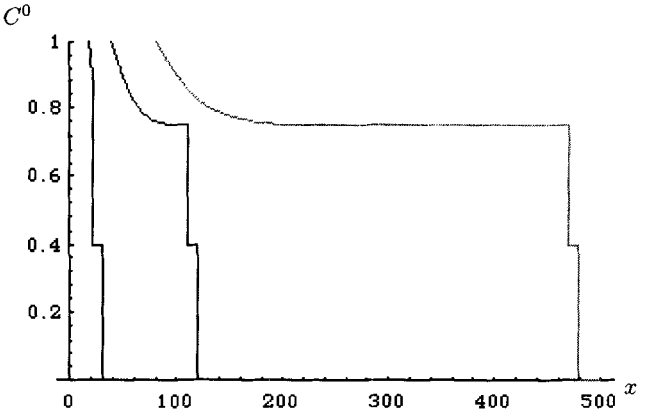

Figure 2. Concentration profiles.

$a = -0.75$, $C_* = 0.4$, $\gamma = 2$, $\alpha = 3$, $\epsilon = 0.0001$, $\kappa = 5$. In decreasing order of darkness: $t = 6$, 24, 96.

Figure 3 shows our large-time asymptotic expansion of σ for the same parameters and times. The gap for $t = 6$ is due to the fact that we are graphing analytical asymptotic expansions. Once again, we see that these expansions do not hold for x near 0; straight lines have been drawn to indicate the value of $\sigma^0(0, t)$ for the times indicated. Note the steep rise of σ over the relatively small scale of the mushy region. Note also that in this case there is no peak in σ, but that the rise in σ is much slower once the polymer entanglement network has begun to dissolve. It is also difficult to ascertain the position of the secondary front from this graph. That is because σ_x^0 is nearly identical on both sides of that front.

For small t, we postulate the following fictitious initial condition as $x \to 0$:

$$C_u(x) \sim C_0 + C_1 x + \frac{C_2 x^2}{2} + \cdots$$

We then perform small-time asymptotics on Eqs. 31–34, keeping only those terms that are $O(t^3)$ and larger. We begin by expanding Eq. 34, which yields

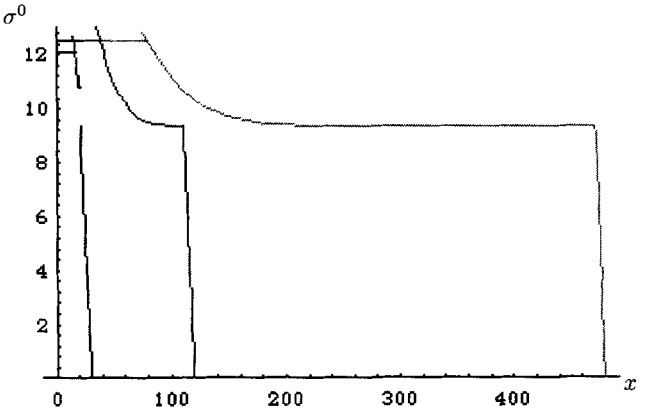

Figure 3. Stress profiles.

$a = -0.75$, $C_* = 0.4$, $\gamma = 2$, $\alpha = 3$, $\epsilon = 0.0001$, $\kappa = 5$. In decreasing order of darkness: $t = 6$, 24, 96.

$$T^{\sigma d} \sim \frac{\kappa x}{\gamma} C_0 + \frac{\kappa x t}{\gamma}\left(\kappa C_1 - \frac{C_0}{2}\right). \tag{52}$$

The integral in $T^{\sigma k}$ does not contribute; the other term is

$$T^{\sigma}(0, t - x/\kappa)e^{-x/2\kappa} \sim \frac{C_* \kappa^2}{\gamma}\left(t - \frac{x}{\kappa}\right) + \frac{\kappa^2 t^2[r(1-C_*) - C_*]}{2\gamma}$$
$$- \frac{\kappa x t}{\gamma}\left[r(1-C_*) - \frac{C_*}{2}\right] - \frac{\kappa^2[r(1-C_*)(1+r) - C_*]t^3}{6\gamma}, \tag{53}$$

where we have used Eq. 26. Substituting Eqs. 52, 53, and 40 into Eq. 12, we have

$$\frac{\kappa^2 C_*}{\gamma}\left(t - \frac{s}{\kappa}\right) = \frac{C_* \kappa^2}{\gamma}\left(t - \frac{s}{\kappa}\right)$$
$$- st\left[r(1-C_*) + \frac{C_0 - C_*}{2} - \kappa C_1\right] + \frac{\kappa t^2[r(1-C_*) - C_*]}{2}$$
$$- \frac{\kappa[r(1-C_*)(1+r) - C_*]t^3}{6} + sC_0. \tag{54}$$

It is clear that the first terms on each side cancel.

We now expand our concentration field for small time, retaining only those terms that are $O(t^2)$ and larger. It can be shown that the integral in T^{cu} is $O(xt)$, so we have

$$T^c(x,t) \sim C_* + tr(1-C_*) + \frac{x}{\kappa}\left[\kappa C_1 - r(1-C_*) + \frac{C_0 - C_*}{2}\right]$$
$$- \frac{r^2 t^2}{2}(1-C_*). \tag{55}$$

Now we use Eq. 55 in Eq. 44. Letting $s(t) = s_0 t^n$, we have (to leading orders)

$$\left\{tr(1-C_*) + \frac{s_0 t^n}{\kappa}\left[\kappa C_1 - r(1-C_*) + \frac{C_0 - C_*}{2}\right] - \frac{r^2 t^2 (1-C_*)}{2}\right\}(\kappa^2 - n^2 s_0^2 t^{2n-2}) - \kappa^2 C_*\left[t - \frac{s_0 t^n}{\kappa}\right]$$
$$= an^2 s_0^2 t^{2n-2}. \tag{56}$$

We must strike a balance among the $O(t)$, $O(t^n)$, and $O(t^{2n-2})$ terms. Choosing $n = 3/2$ induces an $x^{4/3}$ term in our expression for $C_u(x)$. Since we expect that our functional forms will be everywhere twice differentiable with respect to x, we conclude that $n \neq 3/2$. Thus, the $O(t)$ terms must balance one another. This can happen only if

$$r(1-C_*) = C_*. \tag{57}$$

Physically, this mathematical constraint means that in order for our dissolution front to propagate, the concentration at the interface between the polymer and the reservoir must be regulated *by the polymer network itself*. Thus r in some sense represents the internal dissolution rate of the polymer and could be related to the strength of the entanglement network. Similar results have been found experimentally (Hui et al., 1987a).

Using these results in Eq. 56, we have the following (to leading orders):

$$s_0 \kappa t^n\left[\kappa C_1 - C_* + \frac{C_0 - C_*}{2}\right] - \frac{\kappa^2 C_*^2 t^2}{2(1-C_*)}$$
$$+ \kappa C_* s_0 t^n = an^2 s_0^2 t^{2n-2}, \tag{58}$$

from which we have that $n = 2$. Using Eq. 57 in Eq. 54, we have

$$st\left(\kappa C_1 - \frac{C_0 + C_*}{2}\right) - \frac{\kappa r C_* t^3}{6} + sC_0 = 0. \tag{59}$$

So, we may conclude that $C_0 = 0$. Using the fact that $C_0 = 0$ and $n = 2$ in Eq. 58, we have

$$s_0 \kappa\left(\kappa C_1 - \frac{3C_*}{2}\right) + s_0 \kappa C_* - \frac{\kappa^2 C_*^2}{2(1-C_*)} = 4as_0^2. \tag{60}$$

We may combine Eq. 60 with Eq. 59 (using the fact that $C_0 = 0$) to yield

$$s_0 = \frac{\kappa C_*}{2\sqrt{3|a|(1-C_*)}}, \quad C_1 = \frac{C_*}{\kappa}\left[\frac{1}{2} + \sqrt{\frac{|a|}{3(1-C_*)}}\right]. \tag{61}$$

Summarizing our results, we have the following:

$$t \to 0, \quad s(t) \sim \frac{\kappa C_* t^2}{2\sqrt{3|a|(1-C_*)}}, \quad r = \frac{C_*}{1-C_*}, \tag{62a}$$

$$T^c(x,t) \sim \frac{C_* x}{\kappa}\left[\frac{1}{2} + \sqrt{\frac{|a|}{3(1-C_*)}}\right]$$
$$+ [1 - (1-C_*)e^{-r(t - x/\kappa)}]e^{-x/2\kappa} + \frac{x}{2}\int_{x/\kappa}^{t} e^{-z/2}$$
$$\times [1 - (1-C_*)e^{-r(t-z)}]\frac{I_1\left(\sqrt{\kappa^2 z^2 - x^2}/2\kappa\right)}{\sqrt{\kappa^2 z^2 - x^2}} dz, \tag{62b}$$

$$\sigma^{0r}(x,t) \sim \frac{x}{2}\int_{x/\kappa}^{t} e^{-z/2} T^{\sigma}(0, t-z)\frac{I_1\left(\sqrt{\kappa^2 z^2 - x^2}/2\kappa\right)}{\sqrt{\kappa^2 z^2 - x^2}} dz$$
$$+ T^{\sigma}(0, t - x/\kappa)e^{-x/2\kappa} + \frac{C_* e^{-t/2}}{2\gamma}\left[\frac{1}{2} + \sqrt{\frac{|a|}{3(1-C_*)}}\right]$$
$$\times \left[\int_0^{x+\kappa t} z g_d(x-z, t)\, dz - \int_0^{\kappa t - x} z g_d(x+z, t)\, dz\right]. \tag{62c}$$

Figure 4 shows a plot of our superimposed asymptotic expansions for the listed set of parameter values. The gray line

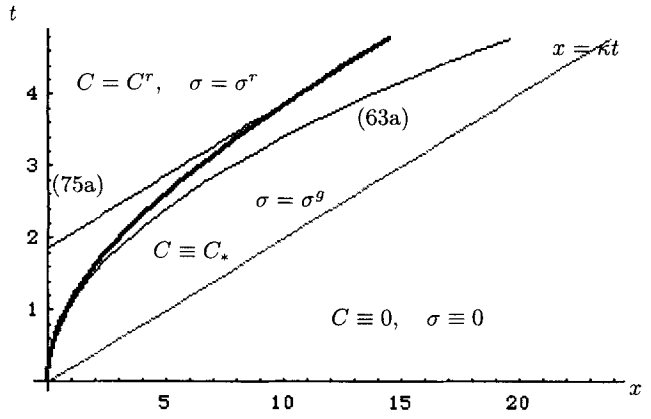

Figure 4. Front diagram with superimposed asymptotic expansions.

$a = -0.75$, $C_* = 0.4$, $\gamma = 2$, $\alpha = 3$, $\epsilon = 0.0001$, $\kappa = 5$.

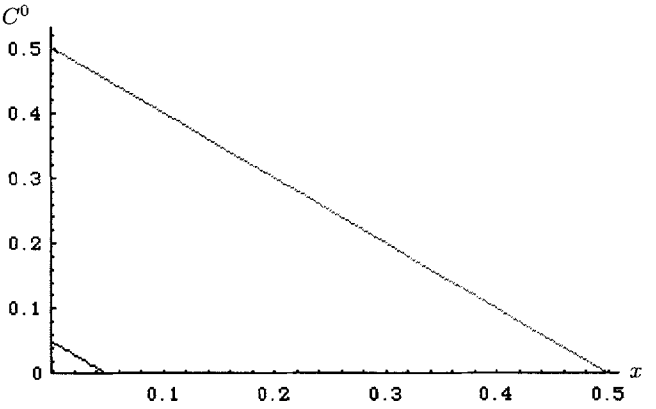

Figure 6. Stress profiles.

$a = -0.75$, $C_* = 0.4$, $\gamma = 2$, $\alpha = 3$, $\epsilon = 0.0001$, $\kappa = 5$. In decreasing order of darkness: $t = 0.001, 0.01, 0.1$.

is the primary front. The narrow lines are the graphs of our actual asymptotic expansions 51a and 62a, while the thicker line is simply a sketch of the way the actual front would interpolate between these two expansions. These graphs indicate a region of finite width where the polymer is in the dissolution process, results seen experimentally by Peppas et al. (1994). In their work, they perform both numerical simulations and experiments of methyl ethyl ketone dissolving polystyrene. Neglecting the effects of swelling, their graphs are qualitatively similar to ours: a leading penetration front moving with constant speed is followed by a dissolution front also moving at the same constant speed, tracking a finite width behind the leading front. Their simulations involved the use of a "dissolution clock"; we have been able to reproduce the result by using the fact that the stress cannot become unbounded.

Note also that there are several important results here from an experimental point of view. By simply performing the experiment heretofore outlined, one can determine κ (from the front speed), C_* (from the concentration in the mushy region), and a (from the width of the mushy region).

Figure 5 shows a graph of C for small times. Note that we have made sure that $\epsilon = o(t)$ for all graphed values. While

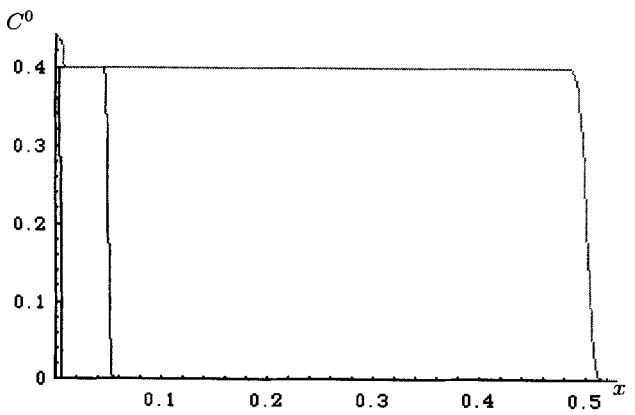

Figure 5. Concentration profiles.

$a = -0.75$, $C_* = 0.4$, $\gamma = 2$, $\alpha = 3$, $\epsilon = 0.0001$, $\kappa = 5$. In decreasing order of darkness: $t = 0.001, 0.01, 0.1$.

difficult to ascertain from the graph for $t = 0.001$, it is clear from the other graphs that we have once again reproduced our three-stage process. The concentration starts out at 0, then rises quickly to C_* at the primary front. C remains at C_* in the mushy region (which for t small is a much larger relative area), and then slowly rises for $x < s(t)$.

Figure 6 shows a graph of σ for the same times and parameter values. The graph for $t = 0.001$ can only be ascertained as an extra pixel in the lower lefthand corner of the graph; the stress is that small for small time. Note that we have linear growth in the mushy region, which now encompasses nearly the entire graph.

Remarks

We have demonstrated that non-Fickian behavior ensues in many polymer-penetrant systems where there is a nonnegligible viscoelastic memory term in the flux. By using perturbation methods to solve the system, we obtain a difficult moving boundary-value problem, which no longer yields to simplistic similarity-variable techniques. Therefore, more sophisticated methods, such as that due to Boley (1961), must be used. The system of integrodifferential equations that results cannot be solved in closed form; thus, an asymptotic solution is expedient. Our solutions indicate several key aspects of these systems.

When the effect of state upon polymer memory is considered, certain non-Fickian traits immediately become evident. We obtain a "dual-front" system, where the polymer is separated by two sharp fronts into regions that are dry, at the dissolution concentration, and nearly saturated. For long times, both of these fronts move with constant speed. These results replicate experiments involving dissolving polymers (Peppas et al., 1994; Wu, 1994).

We choose $a < 0$; therefore, in cases where the stress is important, a cannot be directly related to the latent heat in a Stefan problem. However, note that in our problem $[C_x]_s > 0$. The jump in the standard Fickian flux was positive, as found in a standard Stefan problem; it was the non-Fickian stress contribution to the flux that forced $a < 0$.

We also found another unusual result: the *self-regulating mass uptake* of the dissolving polymer. Perhaps related to the

strength of the entanglement network, this uptake reflects the internal dissolution rate of the polymer. However, note that when we derived an expression for r, we did so having assumed the form of $C(0^+, t)$ as in Eq. 12. Though Eq. 12 is certainly a reasonable first approximation to the actual kinetics at the boundary (Hui et al., 1987a), certainly other forms could be postulated. Uptake models at the boundary incorporating other functional forms would also lead to undetermined constants for which one could solve in a similar fashion to that outlined here.

By properly simplifying the very general equation (Eq. 3) using our physical and mathematical knowledge and intuition about polymer-penetrant systems, we were able to obtain results that replicate several salient features of such systems. By increasing the size of one of our parameters, thereby emphasizing the effects of the nonlinear viscoelastic term, we have obtained fronts that move with constant speed. These fronts, which are sharper than those found in ordinary diffusive systems, have been found experimentally to be characteristic of certain polymer-penetrant systems (Frisch et al., 1969; Fu and Durning, 1993; Hui et al., 1987b).

Acknowledgments

This work was performed under National Science Foundation grant DMS-9024963 and Air Force Office of Scientific Research grant AFOSR-91-0045. Additional support was provided by a National Science Foundation Graduate Fellowship, the John and Fannie Hertz Foundation, and the Theoretical Director's Office and the Center for Nonlinear Studies at Los Alamos National Laboratory. The authors wish to thank Thomas Witelski and Christopher Durning for their contributions, both direct and indirect, to this article. Many of the calculations herein were performed using Maple and Mathematica.

Notation

Units are listed in terms of length (L), mass (M), moles (N), or time (T). The letter with a tilde has dimensions, while the letter without a tilde has none.

a = coefficient in flux-front speed relationship, Eq. 15
$\tilde{C}(\cdot,\tilde{t})$ = concentration of penetrant or diluent at position $\cdot$ and time $\tilde{t}$, units N/L^3
E = coefficient preceding the stress term in the modified diffusion equation, units NT/M, Eq. 2
f = arbitrary function, variously defined
$F(t)$ = integral for asymptotic analysis, Eq. 45
$g(\cdot)$ = kernel in solution representations
$\tilde{J}(\cdot,\tilde{t})$ = flux at position $\cdot$ and time $\tilde{t}$, units N/L^2T
n = indexing variable, Eq. 4, or variable exponent for small-time asymptotics
$\tilde{s}(\tilde{t})$ = position of secondary front, defined as $\tilde{C}(\tilde{s}(\tilde{t}),\tilde{t}) = \tilde{C}_*$, units L, Eq. 13
$\tilde{t}$ = time from imposition of external concentration, units T
$\tilde{x}$ = three-dimensional distance coordinate, units L, Eq. 1
y = dummy integration variable
z = dummy integration variable
Z = the integers

Greek letters

α = nondimensional parameter, value $1+\gamma$, Eq. 16a
ϵ = perturbation expansion parameter, value β_g/β_r, Eq. 16a
κ = nondimensional parameter, value $\sqrt{\eta_0 E/\beta_g D}$, Eq. 16a
$\tilde{\sigma}(\tilde{x},\tilde{t})$ = stress in polymer at position $\tilde{x}$ and time $\tilde{t}$, units M/LT^2, Eq. 1
τ = unstretched boundary-layer variable, analogous to t, Eq. 36
ζ = stretched boundary-layer variable, Eq. 36

Subscripts and superscripts

c = characteristic value of a quantity, Eq. 8; concentration, Eq. 24
d = part of the solution arising from the fictitious Neumann condition, Eq. 34a
$j\epsilon Z$ = term in an expansion, either in t, x, or ϵ
k = part of the solution arising from explicitly known quantities, Eq. 31
u = part of the solution arising from the fictitious Dirichlet condition, Eq. 24
σ = stress, Eq. 24
$-$ = boundary layer in the rubbery region behind the front
$+$ = boundary layer in the glassy region ahead of the front, Eq. 36
$'$ = dummy integration variable, Eq. 1.
$\cdot$ = differentiation with respect to t, Eq. 15 or arbitrary argument
∞ = term in an expansion in t or x
$[\cdot]_{\tilde{s}}$ = jump across the front $\tilde{s}$, defined as ${}^{g}[\tilde{s}^+(\tilde{t}),\tilde{t}] - {}^{r}[\tilde{s}^-(\tilde{t}),\tilde{t}]$

Literature Cited

Abramowitz, M., and I. A. Stegun, eds., *Handbook of Mathematical Functions*, Applied Mathematics Ser., **55**, Nat. Bur. Stand., Washington, DC (1972).
Alfrey, T., E. F. Gurnee, and W. G. Lloyd, "Diffusion in Glassy Polymers," *J. Poly. Sci. C*, **12**, 249 (1966).
Bender, C. M., and S. A. Orszag, *Advanced Mathematical Methods for Scientists and Engineers*, McGraw-Hill, New York (1978).
Boley, B. A., "A Method of Heat Conduction Analysis of Melting and Solidifcation Problems," *J. Math. Phys.*, **40**, 300 (1961).
Christensen, R. M., *Theory of Viscoelasticity*, Academic Press, New York (1971).
Cohen, D. S., and A. B. White, Jr., "Sharp Fronts Due to Diffusion and Stress at the Glass Transition in Polymers," Los Alamos Tech. Rep. 88-2081 (June, 1988); *J. Poly. Sci. B: Poly. Phys.*, **27**, 1731 (1989).
Cohen, D. S., and A. B. White, Jr., "Sharp Fronts Due to Diffusion and Viscoelastic Relaxation in Polymers," *SIAM J. Appl. Math.*, **51**, 472 (1991).
Cohen, D. S., A. B. White, Jr., and T. P. Witelski, "Shock Formation in a Multi-Dimensional Viscoelastic Diffusive System," *SIAM J. Appl. Math.*, **55**, 348 (1995).
Cox, R. W., "A Model for Stress-Driven Diffusion in Polymers," PhD Thesis, Cal. Inst. of Technol., Pasadena (1988).
Cox, R. W., and D. S. Cohen, "A Mathematical Model for Stress-Driven Diffusion in Polymers," *J. Poly. Sci. B: Poly. Phys.*, **27**, 589 (1989).
Cox, R. W., "Shocks in a Model for Stress-Driven Diffusion," *SIAM J. Appl. Math.*, **50**, 1284 (1990).
Crank, J., *The Mathematics of Diffusion*, 2nd ed., Oxford Univ. Press, New York (1976).
Crank, J., *Free and Moving Boundary Problems*, Oxford Univ. Press, New York (1984).
Durning, C. J., "Differential Sorption in Viscoelastic-Fluids," *J. Poly. Sci. B: Poly. Phys.*, **23**, 1831 (1985).
Edwards, D. A., "A Model for Nonlinear Diffusion in Polymers," PhD Thesis, Cal. Inst. of Technol., Pasadena (1994).
Edwards, D. A., "Constant Front Speed in Weakly Diffusive Non-Fickian Systems," *SIAM J. Appl. Math.*, **55**, 1039 (1995).
Edwards, D. A., and D. S. Cohen, "An Unusual Moving Boundary Condition Arising in Anomalous Diffusion Problems," *SIAM J. Appl. Math.*, **55**, 662 (1995a).
Edwards, D. A., and D. S. Cohen, "The Effect of a Changing Diffusion Coefficient in Polymer-Penetrant Systems," *IMA J. Appl. Math.*, **55**, 49 (1995b).
Flugge, W., *Viscoelasticity*, Springer-Verlag, New York (1975).
Frisch, H. L., "Sorption and Transport in Glassy Polymers—A Review," *Poly. Eng. Sci.*, **20**, 2 (1980).
Frisch, H. L., T. K. Kwei, and T. T. Wang, "Diffusion in Glassy Polymers: II," *J. Poly. Sci.*, **7**, 879 (1969).
Fu, T. Z., and C. J. Durning, "Numerical Simulation of Case II Transport," *AIChE J.*, **39**, 1030 (1993).

Hayes, C. K., "Diffusion and Stress Driven Flow in Polymers," PhD Thesis, Cal. Inst. of Tech., Pasadena (1990).
Hayes, C. K., and D. S. Cohen, "The Evolution of Steep Fronts in Non-Fickian Polymer-Penetrant Systems," *J. Poly. Sci. B: Poly. Phys.*, **30**, 145 (1992).
Herman, M. F., and S. F. Edwards, "A Reptation Model for Polymer Dissolution," *Macromolecules*, **23**, 3662 (1990).
Hui, C. Y., K. C. Wu, R. C. Lasky, and E. J. Kramer, "Case II Diffusion in Polymers: I. Transient Swelling," *J. Appl. Phys.*, **61**, 5129 (1987a).
Hui, C. Y., K. C. Wu, R. C. Lasky, and E. J. Kramer, "Case II Diffusion in Polymers: II. Steady State Front Motion," *J. Appl. Phys.*, **61**, 5137 (1987b).
Knauss, W. G., and V. H. Kenner, "On the Hygrothermomechanical Characterization of Polyvinyl Acetate," *J. Appl. Phys.*, **51**, 5131 (1980).
Losi, G.U., and W. G. Knauss, "Free Volume Theory and Nonlinear Thermoviscoelasticity," *Poly. Eng. Sci.*, **32**, 542 (1992).
Martuscelli, E., and C. Marchetta, eds., *New Polymeric Materials: Reactive Processing and Physical Properties*, VNU Science Press, Utrecht, The Netherlands (1987).
Paul, D. R., and W. J. Koros, "Effect of Partially Immobilizing Sorption on Permeability and Diffusion Time Lag," *J. Poly. Sci.*, **14**, 675 (1976).
Peppas, N. A., J. C. Wu, and E. D. von Meerwall, "Mathematical Modeling and Experimental Characterization of Polymer Dissolution," *Macromolecules*, **27**, 5626 (1994).
Pine, A., "Not So Deadly Weapons," *L. A. Times*, Los Angeles (Dec. 18, 1993).
Shimabukuro, S. R., "Stress Assisted Diffusion in Polymers," PhD Thesis, Cal. Inst. of Technol., Pasadena (1990).
Tarche, P. J., *Polymers for Controlled Drug Deliveries*, CRC Press, Boca Raton, FL (1991).
Thomas, N., and A. H. Windle, "A Theory of Case II Diffusion," *Polymer*, **23**, 529 (1982).
Thompson, L. F., C. G. Wilson, and M. J. Bowden, *Introduction to Microlithography*, ACS Symp. Ser., **219** (1983).
Travis, J., "Polymer Gels Get Smarter," *Science*, **259**, 893 (1993).
Vieth, W. R., *Diffusion in and Through Polymers: Principles and Applications*, Oxford Univ. Press, New York (1991).
Vieth, W. R., and K. J. Sladek, "A Model for Diffusion in a Glassy Polymer," *J. Colloid Sci.*, **20**, 1014 (1965).
Vrentas, J. S., C. M. Jorzelski, and J. L. Duda, "A Deborah Number for Diffusion in Polymer-Solvent Systems," *AIChE J.*, **21**, 894 (1975).
Wu, J. C., Quantum Chemical Process Research Center, private communication (Mar. 11, 1994).

Manuscript received May 31, 1994, and revision received Dec. 12, 1994.